

the ether layer separated and dried. To this ether solution was added 2  $\mu\text{L}$  of cyclopentanone as an internal standard, and quantitative analysis by GC gave the concentrations of CyOH and CyONE with time.

**Acknowledgment.** The biomimetic oxidation studies at LBL

were supported by the Electric Power Research Institute under U.S. Department of Energy Contract No. DE-AC03-76SF00098, while the iron cluster synthesis at IU and UL were supported by NSF Grants CHE 8808019 and R11-8610671, respectively.

Contribution from the Department of Chemistry, Amherst College, Amherst, Massachusetts 01002, Departments of Chemistry and Biochemistry and Center for Metalloenzyme Studies, University of Georgia, Athens, Georgia 30602, Lehrstuhl für Mikrobiologie, Universität Karlsruhe, D-7500 Karlsruhe 1, Federal Republic of Germany, and Department of Chemistry, University of Southern California, Los Angeles, California 90089

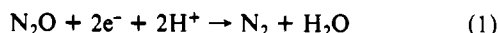
## Spectroscopic Studies of the Copper Sites in Wild-Type *Pseudomonas stutzeri* $\text{N}_2\text{O}$ Reductase and in an Inactive Protein Isolated from a Mutant Deficient in Copper-Site Biosynthesis

David M. Dooley,<sup>\*1</sup> Michele A. McGuirl,<sup>1</sup> Amy C. Rosenzweig,<sup>1</sup> Judith A. Landin,<sup>1</sup> Robert A. Scott,<sup>2</sup> Walter G. Zumft,<sup>3</sup> Frank Devlin,<sup>4</sup> and Philip J. Stephens<sup>4</sup>

Received August 27, 1990

*Pseudomonas stutzeri*  $\text{N}_2\text{O}$  reductase is a complex multicopper enzyme (approximately 8 Cu ions/protein molecule). Two copper sites appear to be closely similar to the  $\text{Cu}_A$ -type site in cytochrome *c* oxidase, but relatively little is known about the other copper sites in  $\text{N}_2\text{O}$  reductase. In this paper circular dichroism, magnetic circular dichroism, and X-ray absorption and fluorescence spectroscopy have been used to further characterize the copper sites in native  $\text{N}_2\text{O}$  reductase and in a "mutant" protein isolated from a strain deficient in the biosynthesis of the  $\text{N}_2\text{O}$  reductase copper sites that contains only 2 copper ions/protein molecule. Both magnetic circular dichroism and X-ray absorption (Cu K-edge and EXAFS) data are consistent with the presence of (on average) one  $\text{Cu}_A$ -type site per protein in the mutant  $\text{N}_2\text{O}$  reductase. Comparisons of the near-infrared circular dichroism spectra of the oxidized native and "mutant"  $\text{N}_2\text{O}$  reductases suggest that transitions at 7200 and 9500  $\text{cm}^{-1}$  in the native enzyme are associated with copper sites other than the  $\text{Cu}_A$ -type sites. To the best of our knowledge, these are the first electronic spectral features that can be attributed to non- $\text{Cu}_A$ -type sites in  $\text{N}_2\text{O}$  reductase. The near-infrared bands are significantly less intense in preparations of  $\text{N}_2\text{O}$  reductase that display lower specific activities. Several electronic transitions are resolved in the circular and magnetic circular dichroism spectra of dithionite-reduced  $\text{N}_2\text{O}$  reductase. Notably a near-infrared band is observed in the circular dichroism spectrum at 8200  $\text{cm}^{-1}$ . The data are plausibly attributed to a highly covalent  $[\text{Cu}(\text{II})-\text{S}(\text{cys}) \leftrightarrow \text{Cu}(\text{I})-\text{S}(\text{cys})]$  site in the reduced enzyme. Copper removal from  $\text{N}_2\text{O}$  reductase enhances the tryptophan fluorescence intensity about 3-fold; most of the quenching appears to be associated with occupation of the  $\text{Cu}_A$ -type sites.

Denitrifying organisms can couple nitrate, nitrite, and nitrous oxide reduction to ATP synthesis,<sup>5</sup> via proton translocation and the formation of a membrane potential.<sup>6</sup>  $\text{N}_2\text{O}$  reductase is generally the terminal enzyme in a complete denitrification pathway; this enzyme catalyzes the two-electron reduction of nitrous oxide (eq 1). The physiological electron donors for various  $\text{N}_2\text{O}$  reductases have not yet been definitively identified, but *c*-type cytochromes are considered likely candidates.<sup>7</sup>



All  $\text{N}_2\text{O}$  reductases isolated to date are complex multicopper enzymes. The enzymes from *Pseudomonas stutzeri*<sup>8-12</sup> and *Paracoccus denitrificans*<sup>13</sup> are the best characterized. Multiple forms of the *P. stutzeri*  $\text{N}_2\text{O}$  reductase have been isolated or prepared; key features of these various forms have been summarized in the literature.<sup>8,9</sup> The native enzyme may be isolated in high-activity or low-activity forms ( $\text{N}_2\text{OR}$  I and  $\text{N}_2\text{OR}$  II, respectively) and contains a maximum of eight copper ions per protein molecule. The *P. stutzeri* protein is a dimer of two identical subunits, and the amino acid sequence has been obtained by translation of the *nosZ* gene in this organism.<sup>14</sup> Comparison of the  $\text{N}_2\text{O}$  reductase sequence to published cytochrome oxidase sequences,<sup>11</sup> together with spectroscopic data,<sup>11,12</sup> strongly indicates that  $\text{N}_2\text{O}$  reductase contains  $\text{Cu}_A$ -type sites. These sites are prominently reflected in the visible absorption spectrum of the resting enzyme (Figure 1). Resonance Raman spectroscopy has shown that the principal electronic absorption band at 540 nm is a  $\text{RS}^-(\text{cys}) \rightarrow \text{Cu}(\text{II})$  ligand-to-metal charge-transfer (LMCT) transition.<sup>10</sup> A  $[\text{Cu}^{\text{II}}(\text{cys}-\text{S})_2(\text{his}-\text{N})_2]$  site is most consistent with the resonance Raman data;<sup>10</sup> a similar coordination environment

has been suggested for  $\text{Cu}_A$  in cytochrome oxidase.<sup>15</sup>  $\text{Cu}_A$  is believed to be located in subunit II of cytochrome oxidase (*coxII*);<sup>16</sup>

- (1) Amherst College.
- (2) University of Georgia.
- (3) Universität Karlsruhe.
- (4) University of Southern California.
- (5) (a) Koike, I.; Hattori, A. *J. Gen. Microbiol.* **1975**, *88*, 11-19. (b) Allen, M. B.; Van Niel, C. B. *J. Bacteriol.* **1952**, *64*, 397-412. (c) Carr, C. J.; Page, M. D.; Ferguson, S. J. *Eur. J. Biochem.* **1989**, *179*, 683-692.
- (6) (a) Boogerd, F. C.; Van Verseveld, H. W.; Stouthamer, A. H. *Biochim. Biophys. Acta* **1981**, *638*, 181-191. (b) Leibowitz, M. R.; Garber, E. A.; Kristjansson, J. K.; Hollocher, T. C. *Curr. Microbiol.* **1982**, *7*, 305-310. (c) McEwan, A. G.; Greenfield, A. J.; Wetzstein, H. G.; Jackson, J. B.; Ferguson, S. J. *J. Bacteriol.* **1985**, *164*, 823-830.
- (7) (a) Payne, W. J. *Denitrification*; Wiley: New York, 1981. (b) Delwiche, C. C., Ed. *Denitrification, Nitrification, and Atmospheric Nitrous Oxide*; Wiley: New York, 1981. (c) Knowles, R. *Microbiol. Rev.* **1982**, *46*, 43-70.
- (8) Coyle, C. L.; Zumft, W. G.; Kroneck, P. M. H.; Körner, H.; Jakob, W. *Eur. J. Biochem.* **1985**, *153*, 459-467.
- (9) Rieger, J.; Zumft, W. G.; Kroneck, P. M. H. *Eur. J. Biochem.* **1989**, *178*, 751-762.
- (10) Dooley, D. M.; Moog, R. S.; Zumft, W. G. *J. Am. Chem. Soc.* **1987**, *109*, 6730-6735.
- (11) Scott, R. A.; Zumft, W. G.; Coyle, C. L.; Dooley, D. M. *Proc. Natl. Acad. Sci. U.S.A.* **1989**, *86*, 4082-4086.
- (12) Jin, H.; Thomann, H.; Coyle, C. L.; Zumft, W. G. *J. Am. Chem. Soc.* **1989**, *111*, 4262-4269.
- (13) Snyder, S. W.; Hollocher, T. C. *J. Biol. Chem.* **1987**, *262*, 6515-6525.
- (14) Viebrock, A.; Zumft, W. G. *J. Bacteriol.* **1988**, *170*, 4658-4668.
- (15) (a) Li, P. M.; Gelles, J.; Chan, S. I.; Sullivan, R. J.; Scott, R. A. *Biochemistry* **1987**, *26*, 2091-2095. (b) Martin, C. T.; Scholes, C. P.; Chan, S. I. *J. Biol. Chem.* **1988**, *263*, 8420-8429. (c) Hoffmann, B. M.; Roberts, J. E.; Swanson, M.; Speck, S. H.; Margoliash, E. *Proc. Natl. Acad. Sci. U.S.A.* **1980**, *77*, 1452-1456. (d) Scott, R. A.; Schwartz, J. R.; Cramer, S. P. *Biochemistry* **1986**, *25*, 5546-5555.
- (16) (a) Holm, L.; Saraste, M.; Wikstrom, M. *EMBO J.* **1987**, *6*, 2819-2823. (b) Steinrück, P.; Steffens, G. C. M.; Panskus, G.; Buse, G.; Ludwig, B. *Eur. J. Biochem.* **1987**, *167*, 431-439.

\* To whom correspondence should be addressed.

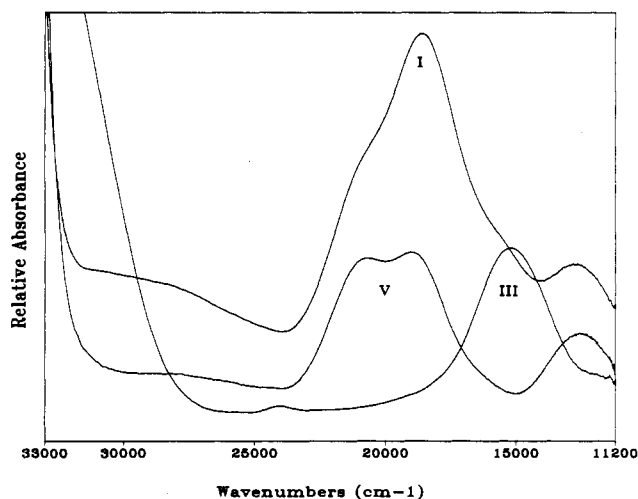


**Figure 1.** Electronic absorption spectra of N<sub>2</sub>O reductase, normalized to protein concentration: I, high-activity, oxidized (resting) form, designated N<sub>2</sub>OR I; III, N<sub>2</sub>OR I following anaerobic reduction by dithionite, designated N<sub>2</sub>OR III; V, modified N<sub>2</sub>O reductase isolated from mutant strain MK402, designated N<sub>2</sub>OR V.

the sequence Gly-X<sub>2</sub>-Cys-Ser-X<sub>2</sub>-Cys-X<sub>3</sub>-His is highly conserved in coxII sequences and is also present in the N<sub>2</sub>O reductase sequence.<sup>11</sup> Recently, a conserved methionine residue in this sequence has been identified.<sup>17</sup> Thus, it seems likely that N<sub>2</sub>O reductase contains two Cu<sub>A</sub>-type sites (one per subunit, on the basis of the sequence).

In contrast, relatively little is known about the other copper sites in this enzyme. Only between 20 and 50% of the copper in resting N<sub>2</sub>O reductase is EPR detectable,<sup>8,9,12</sup> suggesting that Cu(I) sites or antiferromagnetically coupled Cu(II) sites, or both, are present in the oxidized (resting) enzyme. Multiple-frequency EPR spectra are consistent with mixed-valent [Cu(II)-Cu(I)] sites in oxidized N<sub>2</sub>O reductase.<sup>18,19</sup> Interestingly, the dithionite-reduced form of N<sub>2</sub>OR I (designated N<sub>2</sub>OR III) displays an unusually (for copper) broad and unstructured EPR signal, which has about 50% of the total integrated intensity of the initial N<sub>2</sub>OR I form. N<sub>2</sub>OR III also displays an intense ( $\epsilon = 6100 \text{ M}^{-1} \text{ cm}^{-1}$ ) absorption band at 650 nm (Figure 1); the resonance Raman spectrum of this chromophore is similar to blue (type 1) copper spectra.<sup>10</sup> A 650-nm absorption band, associated with a resonance Raman spectrum that is essentially identical with that of N<sub>2</sub>OR III, is also observed in low-activity (N<sub>2</sub>OR II) forms of the resting enzyme. The relationship between the 650-nm chromophores in N<sub>2</sub>OR II and III and the copper sites in the native, high-activity resting form, N<sub>2</sub>OR I, is not known.

Several mutant *P. stutzeri* strains have been isolated that are deficient in N<sub>2</sub>O reductase biosynthesis.<sup>20,21</sup> Three genes, presumably within a single transcriptional unit, have been shown to be required for proper copper incorporation into apo N<sub>2</sub>O reductase. None of these three genes is operative in a transposon Tn5-induced mutant (strain MK402), where it appears that the promoter region has been altered by insertional mutagenesis.<sup>21</sup> An inactive N<sub>2</sub>O reductase, designated N<sub>2</sub>OR V, with an average copper content of only 2 Cu ions/protein molecule, has been purified from this strain.<sup>9,20</sup> Approximately 50% of the copper in N<sub>2</sub>OR V is EPR-nondetectable.<sup>9</sup> The absorption spectrum of N<sub>2</sub>OR V is shown in Figure 1 and suggests that the Cu<sub>A</sub>-type sites might be partially occupied in the "mutant" enzyme.

In this paper we describe the results of spectroscopic studies on various forms of the *P. stutzeri* N<sub>2</sub>O reductase. New electronic

transitions have been observed in the near-infrared region that are probably not associated with the Cu<sub>A</sub>-type sites. X-ray absorption (edge and EXAFS) and CD/MCD spectroscopy have been used to probe the nature of the copper sites in the mutant N<sub>2</sub>O reductase.

### Experimental Procedures

**Materials and Enzymes.** Wild-type N<sub>2</sub>O reductase from *P. stutzeri* ATCC 14405 was purified under anaerobic conditions by procedures previously described<sup>8</sup> and stored in liquid nitrogen until used. Preparations used for the experiments described herein generally had a copper content of  $7 \pm 1$  ions/protein molecule. The purity was checked periodically by SDS and gradient gel electrophoresis and by isoelectric focusing on a Pharmacia PhastSystem. Mutant strain MK402 served as the source of the derivative enzyme, N<sub>2</sub>OR V, which was purified by the same procedure as that for the wild-type enzyme except aerobic conditions were maintained. Owing to its lack of enzymatic activity, N<sub>2</sub>OR V was monitored by immunochemical methods throughout the purification. N<sub>2</sub>OR V was stored in liquid nitrogen prior to use. All chemicals were reagent grade and were used without further purification. Ar gas was purified by passage through an oxygen trap (Chemical Research Supplies). Buffers were prepared from distilled, deionized water or from D<sub>2</sub>O (99.8 atom % D, Aldrich).

**Sample Preparation.** N<sub>2</sub>O reductase samples for spectroscopic experiments in the visible region were in 50 mM Tris buffer, pH 7.5. Generally, beads of the enzyme were removed from liquid-nitrogen storage, thawed, and diluted with ice-cold buffer to a concentration of 0.06–0.12 mM immediately before use. Samples were then allowed to warm to ambient temperature prior to recording their spectra. Samples for near-infrared spectroscopy were in 50 mM Tris buffer, pD 7.9–8.0, prepared by dissolving Tris base in D<sub>2</sub>O and adding DCl (Aldrich) until the measured pH, pH\* = 7.5–7.6. Thawed beads of N<sub>2</sub>O reductase were diluted with deuterated buffer and further equilibrated by at least three concentration/dilution cycles in an ultrafiltration cell (Amicon, YM 30 membrane). Final protein concentrations were as follows: N<sub>2</sub>OR I, 0.30 mM; N<sub>2</sub>OR II, 0.51 mM; N<sub>2</sub>OR III, 0.32 mM; N<sub>2</sub>OR V, 1.08 mM. N<sub>2</sub>OR III was prepared under Ar by adding a 1/30 v/v dithionite solution to give a final dithionite concentration of approximately 9.0 mM. Care was taken to ensure that the copper-depleted N<sub>2</sub>OR V was not exposed to adventitious copper. All buffers were purified over Chelex columns, and glassware (or plasticware) was thoroughly acid-washed. In our experience phosphate buffers are generally preferable to Tris buffers for low-temperature X-ray absorption spectroscopy. Hence, the N<sub>2</sub>OR V sample was dialyzed against 0.1 M potassium phosphate buffer, pH 7.2, and concentrated to approximately 2 mM protein. Samples for fluorescence spectroscopy were 0.025–0.035 mM ( $A_{295} \approx 0.1$ ) in either 25 or 50 mM Tris, pH 7.5. Copper-depleted N<sub>2</sub>O reductase was prepared as follows. A sample of N<sub>2</sub>OR I was reduced anaerobically with 15 equiv (over protein) of dithionite and then dialyzed under Ar against three changes of 25 mM Tris buffer (pH 7.5) containing 10 mM KCN. Cyanide was removed by dialysis (again under Ar) against three changes of Tris buffer. All procedures were carried out at 4 °C.

**Spectroscopy.** Visible CD and MCD spectra were recorded with JASCO J-500 or modified J-40 instruments, as described earlier.<sup>11</sup> A 2-nm spectral bandwidth was maintained. An OLIS Cary-14 and a Cary 219 spectrophotometer interfaced to an IBM PC/AT were used to obtain visible and near-infrared absorption spectra. Near-infrared CD spectra were obtained with a laboratory-constructed instrument that has been described in the literature.<sup>22</sup> Experimental details for the X-ray absorption (edge and EXAFS) measurements were as described in ref 11, except that the copper concentration was 4 mM. The spectral resolution was 0.5 and 1.0 eV for the edge and EXAFS regions, respectively. A Spex Fluorolog photon-counting spectrometer was used for fluorescence spectroscopy. Standard conditions were 1.8-nm band-pass on the excitation and emission monochromators and 0.5-nm steps with 0.5-s integration times. Fluorescence counts were divided by a reference signal generated via a beam splitter and reference photomultiplier to compensate for fluctuations in the lamp output.

### Results

CD spectra of N<sub>2</sub>OR I, N<sub>2</sub>OR III, and N<sub>2</sub>OR V in the visible region are shown in Figure 2. The CD spectrum of N<sub>2</sub>OR II (not shown) is closely similar to that of N<sub>2</sub>OR I. The inset in Figure 2 shows the CD spectrum of another, more concentrated,

(17) Covello, P. S.; Gray, M. W. *FEBS Lett.* **1990**, *268*, 5–7.  
 (18) Kroneck, P. M. H.; Antholine, W. A.; Riestler, J.; Zumft, W. G. *FEBS Lett.* **1988**, *242*, 70–74.  
 (19) Kroneck, P. M. H.; Antholine, W. A.; Kastrau, D. H. W.; Buse, G.; Steffens, G. C. M.; Zumft, W. G. *FEBS Lett.* **1990**, *268*, 274–276.  
 (20) Viebrock, A.; Zumft, W. G. *J. Bacteriol.* **1987**, *169*, 4577–4580.  
 (21) Zumft, W. G.; Viebrock-Sambale, A.; Braun, C. *Eur. J. Biochem.* **1990**, *192*, 591–599.

(22) (a) Osborne, G. A.; Cheng, J. C.; Stephens, P. J. *Rev. Sci. Instrum.* **1973**, *44*, 10–15. (b) Simpkin, D.; Palmer, G.; Devlin, F. J.; McKenna, M. C.; Jensen, G. M.; Stephens, P. J. *Biochemistry* **1989**, *28*, 8033–8039.

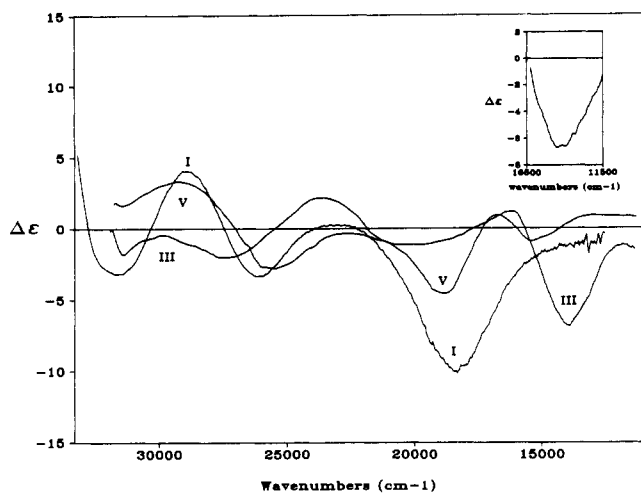


**Figure 2.** Circular dichroism spectra of  $N_2O$  reductase: I, spectrum of the resting, high-activity form,  $N_2OR$  I; III, spectrum of the dithionite-reduced form of  $N_2OR$  I, designated  $N_2OR$  III; V, spectrum of the inactive protein isolated from mutant strain MK402, designated  $N_2OR$  V. Inset: CD spectrum of  $N_2OR$  I in the red region, showing the transition observed by using a more concentrated sample.

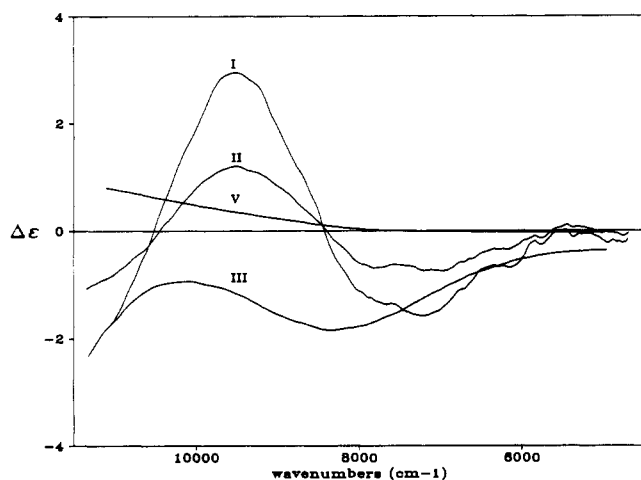


**Figure 3.** Near-infrared circular dichroism spectra of  $N_2O$  reductase: I,  $N_2OR$  I; II, low-activity resting form, designated  $N_2OR$  II; III,  $N_2OR$  III; V,  $N_2OR$  V.

sample of  $N_2OR$  I in the 600–900-nm region ( $16\,667$ – $11\,110\text{ cm}^{-1}$ ). There are several notable features of these spectra. First, the intensities of the  $N_2O$  reductase CD transitions (Figure 2) are quite comparable to those associated with blue (type 1) copper sites,<sup>23</sup> although the dispersions are distinct. Further, these spectra must reflect a number of low-energy electronic transitions in the near-UV and visible regions, consistent with the presence of  $[Cu^{II}(cys-S)_2(his-N)_2]$  sites or other types of  $[Cu^{II}(cys-S)]$  chromophores in  $N_2O$  reductase.<sup>23,24</sup> Finally,  $N_2OR$  I and  $N_2OR$  V have transitions at similar energies throughout the visible region, although the rotational strengths or signs of the bands differ in some cases. Additional transitions are observed in the near-infrared region (Figure 3). The negatively signed intensity above  $10\,000\text{ cm}^{-1}$  in Figure 3 is associated with the lowest energy features evident in Figure 2 (and the inset there). Bands are observed in the near-infrared region at the following energies:  $N_2OR$  I and II,  $9500$  and  $7200\text{ cm}^{-1}$  ( $\sim 1050$  and  $1390\text{ nm}$ );

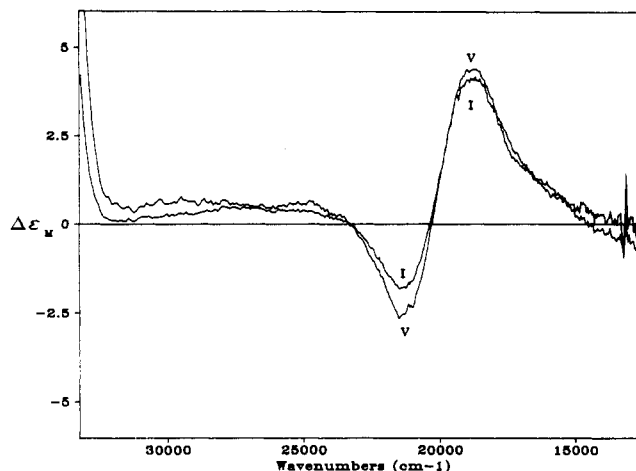


**Figure 4.** Comparison of the room-temperature, visible-region MCD spectra of native  $N_2O$  reductase ( $N_2OR$  I) and the mutant enzyme ( $N_2OR$  V): I,  $N_2OR$  I; V,  $N_2OR$  V. Each spectrum has been normalized to the paramagnetic copper content of the sample.

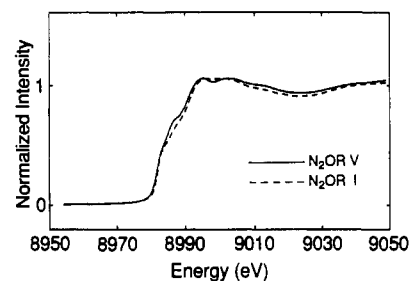


**Figure 5.** Copper K-edge X-ray absorption spectra of the native ( $N_2OR$  I) and mutant ( $N_2OR$  V)  $N_2O$  reductases, normalized to unit edge jump.

$N_2OR$  III,  $8200\text{ cm}^{-1}$  ( $\sim 1220\text{ nm}$ ). The intensities of the  $N_2OR$  II bands are approximately half those of  $N_2OR$  I. Unexpectedly, no near-infrared transitions were detected for  $N_2OR$  V. Numerous studies have established that  $Cu(II)$  complexes with near-tetrahedral geometries display ligand field transitions in the near-infrared region.<sup>23,24</sup> For example, type 1  $Cu(II)$  sites typically display near-infrared transitions at  $5000$ – $6000\text{ cm}^{-1}$  ( $2000$ – $1667\text{ nm}$ ),  $8000$ – $10\,000\text{ cm}^{-1}$  ( $1250$ – $1000\text{ nm}$ ), and  $11\,000$ – $14\,000\text{ cm}^{-1}$  ( $\sim 900$ – $700\text{ nm}$ ). Therefore, the bands observed in the near-infrared CD spectra of  $N_2O$  reductase samples may be plausibly assigned as  $Cu(II)$  d–d transitions, at least for  $N_2OR$  I and  $N_2OR$  II.

Figure 4 compares the visible MCD spectra of  $N_2OR$  I and  $N_2OR$  V.  $N_2OR$  I contains two  $Cu_A$ -type sites, although these sites may not be fully occupied. Recent low-temperature MCD<sup>25</sup> and magnetic susceptibility<sup>26</sup> measurements indicate that the  $Cu_A$  centers, which dominate the MCD spectrum,<sup>11,25</sup> can account for all the observed paramagnetism of native  $N_2O$  reductase at pH 7.5. Therefore, the MCD spectra in Figure 4 have been normalized to the paramagnetic copper content of the samples. Clearly, the normalized MCD spectra of  $N_2OR$  I and  $N_2OR$  V are closely similar.

The copper sites in the “mutant”  $N_2O$  reductase have also been characterized by X-ray absorption spectroscopy (XAS). Copper K-edge spectra of  $N_2OR$  V and  $N_2OR$  I are shown in Figure 5. These spectra are clearly very similar, but minor differences are apparent, especially a slight shift to lower energy in  $N_2OR$  V compared to  $N_2OR$  I. Copper EXAFS data for  $N_2OR$  I and  $N_2OR$  V as well as the associated Fourier transforms are displayed in Figure 6. Much greater differences between  $N_2OR$  V and  $N_2OR$  I are apparent, particularly in the  $k = 7$ – $11\text{ \AA}^{-1}$  range, where  $N_2OR$  V has considerably more amplitude. This is reflected in the FT, where it is clear that the  $R' = 1.9\text{ \AA}$  peak has increased

(23) (a) Solomon, E. I.; Penfield, K. W.; Wilcox, D. E. *Struct. Bonding (Berlin)* **1983**, *53*, 1–57. (b) Dooley, D. M.; Dawson, J. H. *Coord. Chem. Rev.* **1984**, *60*, 1–66. (c) Solomon, E. I.; Hare, J. W.; Dooley, D. M.; Dawson, J. H.; Stephens, P. J.; Gray, H. B. *J. Am. Chem. Soc.* **1980**, *102*, 168–178. (d) Penfield, K. W.; Gay, R. R.; Himmelwright, R. S.; Eickman, N. C.; Norris, V. A.; Freeman, H. C.; Solomon, E. I. *J. Am. Chem. Soc.* **1981**, *103*, 4382–4388.

(24) Lever, A. B. P. *Inorganic Electronic Spectroscopy*, 2nd ed.; Elsevier: Amsterdam, 1984.

(25) Thomson, A. J.; Dooley, D. M. Unpublished results.

(26) Day, E. P.; Dooley, D. M. Unpublished observations.

Table I. Curve-Fitting Results for the First Coordination Sphere of N<sub>2</sub>O Reductase Derivatives<sup>a</sup>

sample	fit	Cu(N,O)			Cu(S,Cl)			<i>f</i> <sup>b</sup>
		<i>N</i> <sub>s</sub>	<i>R</i> <sub>ss</sub> , Å	$\Delta\sigma_{ss}^2$ , Å <sup>2</sup>	<i>N</i> <sub>s</sub>	<i>R</i> <sub>ss</sub> , Å	$\Delta\sigma_{ss}^2$ , Å <sup>2</sup>	
N <sub>2</sub> OR I	1	(3.0) <sup>c</sup>	1.99	+0.0054	(1.0)	2.27	-0.0004	0.059
	2	(1.0)	1.86	+0.0027	(1.0)	2.27	-0.0018	0.052
		(2.0)	2.00	-0.0005				
	3	(2.5)	1.99	+0.0046	(1.0)	2.26	+0.0002	0.011
N <sub>2</sub> OR V	4	(1.0)	1.90	+0.0006	(1.0)	2.27	-0.0007	0.007
		(1.5)	2.03	-0.0011	(0.5)	2.60	+0.0006	
	5	1.99	2.01	(+0.0046)	1.47	2.27	(+0.0002)	0.009
					0.83	2.59	(0.0000)	
	6	0.35	1.90	(+0.0006)	1.47	2.27	(-0.0007)	0.006
		1.15	2.02	(-0.0011)	0.83	2.59	(+0.0006)	

<sup>a</sup>*N*<sub>s</sub> is the number of scatterers per copper; *R*<sub>ss</sub> is the copper-scatterer distance;  $\Delta\sigma_{ss}^2$  is a relative mean-square deviation in *R*<sub>ss</sub>, with  $\Delta\sigma_{ss}^2 = \sigma_{ss}^2(\text{sample}) - \sigma_{ss}^2(\text{model})$ . The model compounds are as follows: Cu(II)-N, [Cu(imid)<sub>4</sub>]<sup>2+</sup> at 4 K; Cu(II)-S, [Cu(mnt)<sub>2</sub>]<sup>2-</sup> at 4 K. <sup>b</sup>*f*<sup>b</sup> is a goodness-of-fit statistic normalized to the overall magnitude of the *k*<sup>3</sup> $\chi(k)$  data:

$$f^b = \frac{[\sum [k^3(\chi_{\text{obsd}}(i) - \chi_{\text{calc}}(i))]^2 / N]^{1/2}}{(k^3\chi)_{\text{max}} - (k^3\chi)_{\text{min}}}$$

<sup>c</sup>Numbers in parentheses were not varied during optimization.

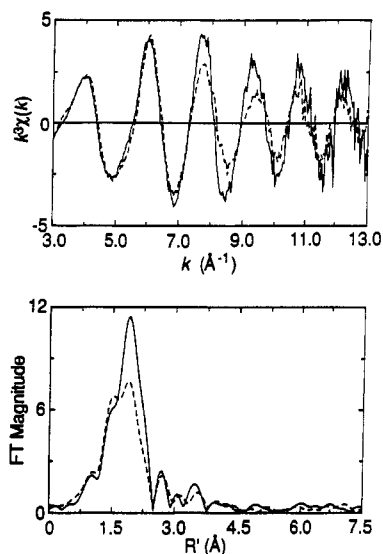


Figure 6. Copper EXAFS data and Fourier transforms for oxidized high-activity N<sub>2</sub>O reductase (N<sub>2</sub>OR I) and the oxidized mutant protein (N<sub>2</sub>OR V): (A, top) EXAFS data for N<sub>2</sub>OR V (—) and N<sub>2</sub>OR I (---) (B, bottom) Fourier transforms over the *k* = 3.0–13.0 Å<sup>-1</sup> range (*k*<sup>3</sup> weighting) of the data in A for N<sub>2</sub>OR V (—) and N<sub>2</sub>OR I (---).

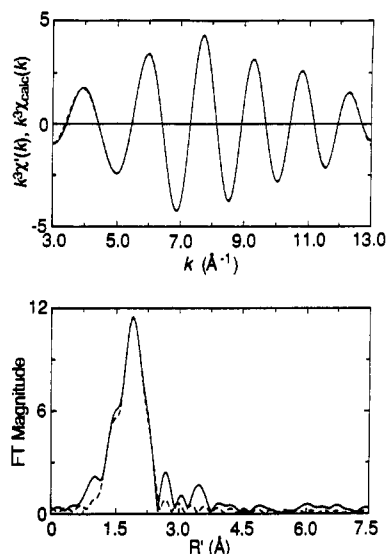


Figure 7. Curve-fitting simulation for the N<sub>2</sub>OR V EXAFS. The first shell peak (*R*' = 1.10–2.50 Å) of the Fourier transform data was back-transformed to yield the filtered EXAFS data shown as the solid line. The dashed line represents the best curve-fitting simulation (fit 6, Table I).

in amplitude. EXAFS curve-fitting analyses for both N<sub>2</sub>OR I and N<sub>2</sub>OR V are set out in Table I, and the best fit is compared to the filtered data in Figure 7. N<sub>2</sub>OR V curve-fitting was performed by assuming that the same types of scatterer shells are present as in N<sub>2</sub>OR I; Debye–Waller factors for each type of scattering shell were fixed at the N<sub>2</sub>OR I values for that shell. The number, *N*<sub>s</sub>, of scattering atoms in each shell was varied in the optimizations for N<sub>2</sub>OR V. As previously established for N<sub>2</sub>OR I,<sup>11</sup> Cu–(S,Cl) interactions at 2.27 and 2.59 Å are required to fit the N<sub>2</sub>OR V EXAFS. Note, however, that the number of (S,Cl) scatterers is increased, and the number of (N,O) scatterers decreased, in N<sub>2</sub>OR V relative to N<sub>2</sub>OR I. Another interesting feature of these fits is that the 2.59-Å Cu–(S,Cl) interactions appear to scale with the 2.27-Å Cu–(S,Cl); i.e., there are consistently about half as many of the longer scatterers. At this time we have not attempted to fit any of the features attributable to second- and third-shell scattering with a Cu–Cu interaction, primarily because we wish to obtain data on an independent sample to ensure that all such features are fully reproducible. Hence, the current EXAFS analysis does not preclude the possibility that significant Cu–Cu interactions may be present.

Fluorescence spectroscopy has been used to check possible interactions between aromatic residues and the copper centers in

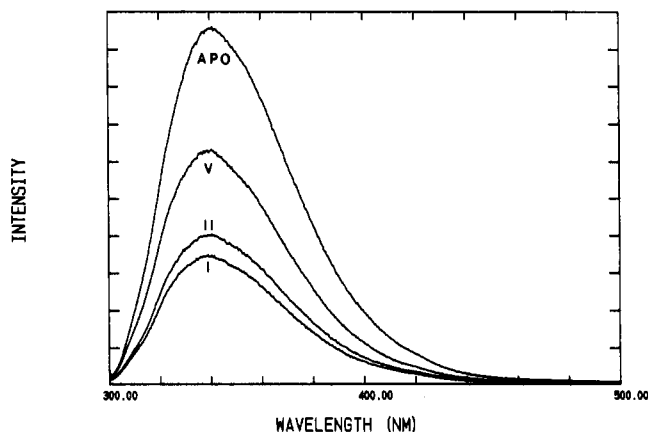


Figure 8. Fluorescence spectra of various forms of N<sub>2</sub>O reductase, obtained with 295-nm excitation: I, N<sub>2</sub>OR I; II, N<sub>2</sub>OR II; V, N<sub>2</sub>OR V; Apo, copper-depleted N<sub>2</sub>OR I.

N<sub>2</sub>O reductase. Fluorescence spectra, obtained with 295-nm excitation, of various forms of N<sub>2</sub>O reductase are displayed in Figure 8. Because the excitation wavelength was 295 nm, tyrosine

residues make practically no contribution to the protein fluorescence spectra shown in Figure 8. Copper binding dramatically quenches the tryptophan fluorescence of apo N<sub>2</sub>O reductase. The N<sub>2</sub>OR V fluorescence intensity is approximately midway between that of N<sub>2</sub>OR I and the apo protein, which roughly correlates with its Cu<sub>A</sub> content (vide infra). Much of the quenching might therefore be associated with copper binding at the Cu<sub>A</sub>-type site. If so, this implies that the neighboring tryptophan residues are efficient energy acceptors. N<sub>2</sub>OR I and N<sub>2</sub>OR II have similar tryptophan fluorescence spectra, but the somewhat greater intensity of N<sub>2</sub>OR II is consistently observed and maintained when the fluorescence is excited at 280 nm (data not shown).

### Discussion

We have previously described evidence from X-ray absorption and MCD spectroscopy that is consistent with the presence of Cu<sub>A</sub>-type sites in native N<sub>2</sub>O reductase.<sup>11</sup> Comparisons to published cytochrome oxidase subunit II (cox II) sequences revealed significant homology between a 15-residue N<sub>2</sub>O reductase sequence and the cox II sequences containing the Cu<sub>A</sub> binding site from several organisms.<sup>11</sup> Thorough studies of N<sub>2</sub>O reductase by cw-EPR spectroscopy<sup>18,19</sup> and pulsed-EPR spectroscopy<sup>12</sup> have provided independent evidence for Cu<sub>A</sub>-type sites in resting N<sub>2</sub>O reductase. Some key spectroscopic or physical signatures for Cu<sub>A</sub> include (1) the MCD spectrum, which is conspicuously different from the MCD spectra of other types of Cu(II) sites,<sup>23</sup> (2) the copper X-ray absorption edge, (3) the 2.27- and 2.6-Å Cu-(S,Cl) interactions and (4) the electron spin-echo envelope modulation pattern, which also appears unique among Cu(II) proteins.<sup>12</sup> The association of the seven-line EPR signal, which is characteristic of N<sub>2</sub>OR I, with the Cu<sub>A</sub> site has been more controversial,<sup>27</sup> principally owing to the emerging evidence that the seven-line signal is most consistent with a mixed-valence  $S = 1/2$  [Cu(1.5)-Cu(1.5)] center.<sup>19</sup> This view is at odds with widely accepted models for Cu<sub>A</sub>.<sup>27</sup>

Collectively the data presented in Figures 4–6 and Table I strongly suggest that the “mutant” enzyme, N<sub>2</sub>OR V, also contains an occupied Cu<sub>A</sub>-type site. The intensity of the MCD spectrum suggests that, on average, the N<sub>2</sub>OR V protein contains one Cu<sub>A</sub>-type Cu(II).<sup>28</sup> EXAFS curve-fitting analyses (Table I, Figure 6) are fully consistent with a higher percentage of the total copper in N<sub>2</sub>OR V being Cu<sub>A</sub> type. Riester et al. have previously pointed out that the EPR parameters, particularly the *g* values, of N<sub>2</sub>OR V suggest it has an electronic environment similar to that of Cu<sub>A</sub>.<sup>9</sup> N<sub>2</sub>OR V also displays the characteristic multiline EPR signals at S-, C-, and X-band observed for N<sub>2</sub>OR I.<sup>19</sup> Kroneck et al. have recently suggested that the mixed-valence site may be the main copper site in N<sub>2</sub>OR V.<sup>19</sup>

It is important to recognize that the primary structure of N<sub>2</sub>OR V is identical with that of the native enzyme; the structural gene (*nosZ*) is transcribed normally in strain MK402, from which N<sub>2</sub>OR V has been isolated. During purification N<sub>2</sub>OR V behaves very similarly to the wild-type enzyme. Furthermore, N<sub>2</sub>OR V is immunochemically and electrophoretically identical with the copper-depleted form of N<sub>2</sub>OR I. N<sub>2</sub>OR V is also translocated across the cytoplasmic membrane into the periplasmic space, where the wild-type enzyme functions. Hence, it is plausible that the tertiary structures of N<sub>2</sub>OR V and N<sub>2</sub>OR I are at least similar. Recent evidence indicates that full copper incorporation into *P. stutzeri* N<sub>2</sub>O reductase requires three, possibly four, genes in addition to *nosZ*.<sup>21</sup> The proteins coded by these genes are probably

involved in copper processing or insertion and appear to be specific for N<sub>2</sub>O respiration. To our knowledge, N<sub>2</sub>O reductase is the first copper enzyme for which a strong case can be made that metal binding to the apo protein is enabled, assisted, or catalyzed by additional proteins. In strain MK402 three of these genes, those downstream of *nosZ*, are not functional so that only copper incorporation that is independent of these proteins can occur. In this context, it may be significant that purified N<sub>2</sub>OR V does not bind added copper.<sup>9</sup> For these reasons we believe that it is important to characterize the copper sites in the purified “mutant” protein, N<sub>2</sub>OR V.

The similarity of the room-temperature MCD spectra, the XAS features, and the EPR spectra suggests that the electronic structures of the Cu<sub>A</sub>-type site in N<sub>2</sub>OR I and the paramagnetic center in N<sub>2</sub>OR V are also similar. On the other hand, the absorption spectra of N<sub>2</sub>OR I and N<sub>2</sub>OR V are not identical (Figure 1).<sup>28</sup> In fact, the N<sub>2</sub>OR V spectrum resembles that of wild-type N<sub>2</sub>O reductase following copper removal and reconstitution;<sup>9</sup> the reconstituted protein is also catalytically inactive. Moreover, the visible CD spectra of N<sub>2</sub>OR V and N<sub>2</sub>OR I differ with regard to rotational strength and sign below 20 000 cm<sup>-1</sup>. Such effects may be attributed to differences in the coupling between the dissymmetric protein matrix and the Cu(II) electronic states, especially since the energies of the various transitions in the spectra of N<sub>2</sub>OR I and N<sub>2</sub>OR V do not appear to be very different. Alternatively, the differences between the absorption and CD spectra of N<sub>2</sub>OR I and N<sub>2</sub>OR V may reflect the contributions from copper sites that simply are not occupied in the mutant protein. On balance the evidence indicates that a Cu<sub>A</sub>-type site (possibly somewhat perturbed) is present in N<sub>2</sub>OR V, but the structural basis for any differences in the Cu<sub>A</sub>-type sites in N<sub>2</sub>OR I and N<sub>2</sub>OR V cannot yet be defined.

The conclusion that N<sub>2</sub>OR V probably contains an occupied Cu<sub>A</sub>-type site may have important consequences for interpreting the near-infrared CD spectra of both N<sub>2</sub>OR V and N<sub>2</sub>OR I. Clearly the signal-to-noise ratio in Figure 3 is sufficient to exclude the possibility that the bands at 7200 and 9500 cm<sup>-1</sup> (~1390 and 1050 nm) were not observed in the N<sub>2</sub>OR V spectrum owing to the lower absolute content of Cu<sub>A</sub>-type sites in N<sub>2</sub>OR V. Since the *g* values of N<sub>2</sub>OR I and N<sub>2</sub>OR V are close in magnitude, the ligand-field transitions of the paramagnetic sites in these proteins should be observed at approximately the same energies. This idea is supported by the close correspondence in the energies of the LMCT transitions between N<sub>2</sub>OR I and N<sub>2</sub>OR V; for example, the principal LMCT transition in N<sub>2</sub>OR I is at 18 620 cm<sup>-1</sup> (537 nm) compared to 18 900 cm<sup>-1</sup> (526 nm) in N<sub>2</sub>OR V (Figure 1). It follows that the presence of the near-infrared CD bands in N<sub>2</sub>OR I and N<sub>2</sub>OR II, and their absence in N<sub>2</sub>OR V, suggest that Cu(II) sites *other than the Cu<sub>A</sub>-type sites* are associated with the transitions at 7200 and 9500 cm<sup>-1</sup>.<sup>29</sup> There are few, if any, other electronic spectral features that may be attributed to the non-Cu<sub>A</sub>-type sites in N<sub>2</sub>O reductase. This result, together with the observation of a near-infrared transition for N<sub>2</sub>OR III, suggests that near-infrared CD spectroscopy will be an informative probe of the active-site structure and reactions of N<sub>2</sub>O reductase.

The structures of the paramagnetic blue ( $\lambda_{\text{max}} = 650$  nm) chromophores in N<sub>2</sub>OR III and N<sub>2</sub>OR II are problematic. As noted previously,<sup>8</sup> the EPR spectrum of N<sub>2</sub>OR III is very unusual, particularly for a Cu(II) site. This signal is present to a variable extent in N<sub>2</sub>OR II as well. However, the resonance Raman spectrum of the 650-nm chromophore is similar to the resonance Raman spectra of blue copper proteins.<sup>10</sup> For this reason it was suggested that N<sub>2</sub>OR II and N<sub>2</sub>OR III contained a copper site (or sites) that is (are) similar to a classical blue copper site and perhaps very inaccessible to external reductants.<sup>10</sup> Riester et al. showed that the blue chromophore in N<sub>2</sub>OR III could not be

(27) (a) Li, P. M.; Malmström, B. G.; Chan, S. I. *FEBS Lett.* **1989**, *248*, 210–211. (b) Kroneck, P. M. H.; Antholine, W. A.; Riester, J.; Zumft, W. G. *FEBS Lett.* **1989**, *248*, 212–213.

(28) The intensity of the principal electronic absorption band ( $\lambda_{\text{max}} = 540$  nm) of N<sub>2</sub>O reductase varies significantly from preparation to preparation and is sensitive to a variety of laboratory factors. Hence, it is a less reliable measure of the Cu<sub>A</sub> content. The oscillator strengths of ligand-to-metal charge-transfer transitions depend upon ground-state and excited-state covalency<sup>23,24</sup> and can readily vary by a factor of 2 or more in response to minor structural perturbations. This seems, for example, to be the case in blue copper (type 1) proteins.

(29) It is possible that the rotational strengths of the near-infrared transitions in N<sub>2</sub>OR V are much smaller than those in N<sub>2</sub>OR I. In order for the transitions to go undetected under our conditions, the difference in rotational strengths in the near-infrared region would have to be significantly greater than the differences evident in the visible region (Figure 2).

reduced by any of several strong reducing agents with varied structures and net charges.<sup>9</sup> They suggested that the spectroscopic and chemical properties of the blue chromophore in N<sub>2</sub>OR III might be consistent with its formulation as a [Cu(I)-SR<sup>+</sup>] site "stabilized" by additional sulfur ligation.<sup>9</sup> These suggestions concerning the nature of the blue N<sub>2</sub>O reductase center are not necessarily inconsistent, since [Cu(II)-SR<sup>-</sup>] and [Cu(I)-SR<sup>+</sup>] may simply be resonance forms describing a highly covalent paramagnetic site. Such considerations have been raised in discussions of the Cu<sub>A</sub> site in cytochrome oxidase.<sup>15</sup> Certainly the number, intensities, and energies of the transitions observed in the visible and near-infrared CD spectra of N<sub>2</sub>OR III are consistent with formulating the blue chromophore as a near-tetrahedral [Cu(II)-SR<sup>-</sup>] site, most probably with pronounced delocalization. On the basis of our data, we cannot unequivocally distinguish between the limiting possibilities, since too little is known about the electronic properties of copper(I)-thiyl radicals.

N<sub>2</sub>O reductase contains nine tryptophans per subunit; five of these are in the carboxyl-terminal half of the protein, which contains the Cu<sub>A</sub>-type site. Two tryptophan residues are located within two or three residues of a conserved cysteine (cys-618), which is part of the presumed Cu<sub>A</sub> site. The tryptophan fluorescence quenching (Figure 8) in N<sub>2</sub>OR I and N<sub>2</sub>OR V, relative to the apo protein, is pronounced and seems to correlate with the Cu<sub>A</sub> content rather than the total copper content. This

suggests that the Cu<sub>A</sub>-type sites may form a "fluorescence-energy sink" when occupied. Such a result would not be unexpected given the paramagnetism and the number of low-energy electronic states associated with these sites. It remains to be seen if the fluorescence is sensitive to the redox state of the Cu<sub>A</sub>-type sites or other copper sites in N<sub>2</sub>O reductase. The initial results do suggest that fluorescence spectroscopy will be useful in studies of N<sub>2</sub>O reductase and that additional studies are warranted.

**Acknowledgment.** This research was supported by the Cooperative State Research Service, U.S. Department of Agriculture, under Agreements 87-CRCR-1-2477 and 89-37280-4696 (to D.M.D.), the National Science Foundation (Grant DMB 86-45819 to R.A.S.), the Deutsche Forschungsgemeinschaft and Fonds der Chemischen Industrie (W.G.Z.), and the NIH (Grant GM 28386 to P.J.S.). The X-ray absorption spectroscopy reported herein was performed at the Stanford Synchrotron Radiation Laboratory, which is operated by the Department of Energy, Division of Chemical Sciences. The SSRL Biotechnology program is supported by the National Institutes of Health Biomedical Resource Technology Program, Division of Research Resources. R.A.S. acknowledges a National Science Foundation Presidential Young Investigator Award.

**Registry No.** Cu, 7440-50-8; N<sub>2</sub>O reductase, 55576-44-8; Cys, 52-90-4.

Contribution from the Department of Chemistry and Biochemistry, Utah State University, Logan, Utah 84322-0300, and Departments of Chemistry and Nutrition and Food Sciences, University of Arizona, Tucson, Arizona 85721

## Stoichiometry of Electron Uptake and the Effect of Anions and pH on the Molybdenum and Heme Reduction Potentials of Sulfite Oxidase

Jack T. Spence,<sup>1a</sup> Cary A. Kipke,<sup>1b,†</sup> John H. Enemark,<sup>\*,1b</sup> and Roger A. Sunde<sup>1c,‡</sup>

Received October 9, 1990

Microcoulometric titrations of chicken liver sulfite oxidase under varied conditions at 25 °C have shown that the enzyme requires three electrons for complete subunit reduction. Reduction potentials (vs NHE) for the molybdenum site at pH 9.00 in the absence of coordinating anions (Mo(VI/V) = 0.057 V, Mo(V/IV) = -0.233 V) are considerably more negative than at pH 6.00 in 0.10 M KCl (Mo(VI/V) = 0.131 V, Mo(V/IV) = -0.086 V), consistent with the formation of chloride complexes of the Mo(V) and Mo(IV) states. Phosphate (H<sub>2</sub>PO<sub>4</sub><sup>-</sup>) competes effectively with chloride for the Mo(V) site of the enzyme at lower concentrations (0.020 M phosphate vs 0.10 M KCl, pH 7.00) and complexes the Mo(VI) state, as seen in the significant negative shifts of the reduction potentials (Mo(VI/V) = 0.038 V, Mo(V/IV) = -0.239 V). Dissociation constants for proton and phosphate complexes of the Mo(VI) state and the chloride complex of the Mo(IV) state have been estimated. The heme reduction potentials decrease with increase in pH and are relatively unaffected by anions. The results are consistent with the results of recent EPR and EXAFS studies of the enzyme regarding active-site structure.

### Introduction

Sulfite oxidase (sulfite: ferricytochrome *c* oxidoreductase EC 8.1.2.1) is a dimeric enzyme that contains one molybdopterin center and one cytochrome *b*<sub>5</sub> type heme in each monomeric subunit.<sup>2,3</sup> The enzyme catalyzes the physiologically important oxidation of sulfite to sulfate, with the oxidation of substrate occurring at the molybdenum center.<sup>4-6</sup> The postulated catalytic cycle for the enzyme requires a two-electron change in the oxidation state of the molybdenum site (Mo(VI)/(Mo(IV))) and a one-electron change in the oxidation state of the heme site (Fe(III)/Fe(II)).<sup>4,7</sup> Data for the electron uptake of sulfite oxidase have not been previously reported. Electron uptake results for both nitrate reductase (*Chlorella vulgaris*) and milk xanthine oxidase, obtained by microcoulometry, show that their molybdenum centers are reduced by two electrons.<sup>8,9</sup>

The heme reduction potentials for the chicken liver and beef liver enzymes have been previously measured at room temperature by spectroelectrochemical titration at pH 7.00 in the presence of

chloride and phosphate ions.<sup>10,11</sup>

The molybdenum reduction potentials for the beef liver enzyme have been previously determined by potentiometric titration using low-temperature EPR spectroscopy at pH 7.00 and 9.00 in the

- (1) (a) Utah State University. (b) Department of Chemistry, University of Arizona. (c) Department of Nutrition and Food Sciences, University of Arizona.
- (2) Cohen, H. J.; Fridovich, I.; Rajagopalan, K. V. *J. Biol. Chem.* **1971**, *246*, 374.
- (3) Cohen, H. J.; Fridovich, I. *J. Biol. Chem.* **1971**, *246*, 367.
- (4) Rajagopalan, K. V. In *Molybdenum and Molybdenum Containing Enzymes*; Coughlan, M. P., Ed.; Pergamon: Oxford, England, 1980; p 243.
- (5) Johnson, J. L.; Cohen, H. J.; Rajagopalan, K. V. *J. Biol. Chem.* **1974**, *249*, 5046.
- (6) Johnson, J. L.; Rajagopalan, K. V.; Cohen, H. J. *J. Biol. Chem.* **1974**, *249*, 859.
- (7) Garner, C. D.; Buchanan, I.; Collison, D.; Mabbs, F. E.; Porter, T. G.; Wynn, C. H. In *Proceedings From the Fourth International Conference on the Chemistry and Uses of Molybdenum*; Barry, H. F., Mitchell, P. C. H., Eds.; Climax Molybdenum Co.: Ann Arbor, MI, 1982; p 163.
- (8) Spence, J. T.; Barber, M. J.; Solomonson, L. P. *Biochem. J.* **1988**, *250*, 921.
- (9) Spence, J. T.; Barber, M. J.; Siegel, L. M. *Biochem.* **1982**, *21*, 1656.
- (10) Barber, M. J.; Kay, C. J. *Fed. Proc.* **1988**, *47*, 843.
- (11) Cramer, S. P.; Gray, H. B.; Scott, N. S.; Barber, M.; Rajagopalan, K. V. In *Molybdenum Chemistry of Biological Significance*; Newton, W. E., Otsuka, S., Eds.; Plenum: New York, 1980; p 157.

\* To whom correspondence should be addressed.

† Current address: CDI/3M Health Care, Tustin, CA.

‡ Current address: University of Missouri, Columbia, MO.